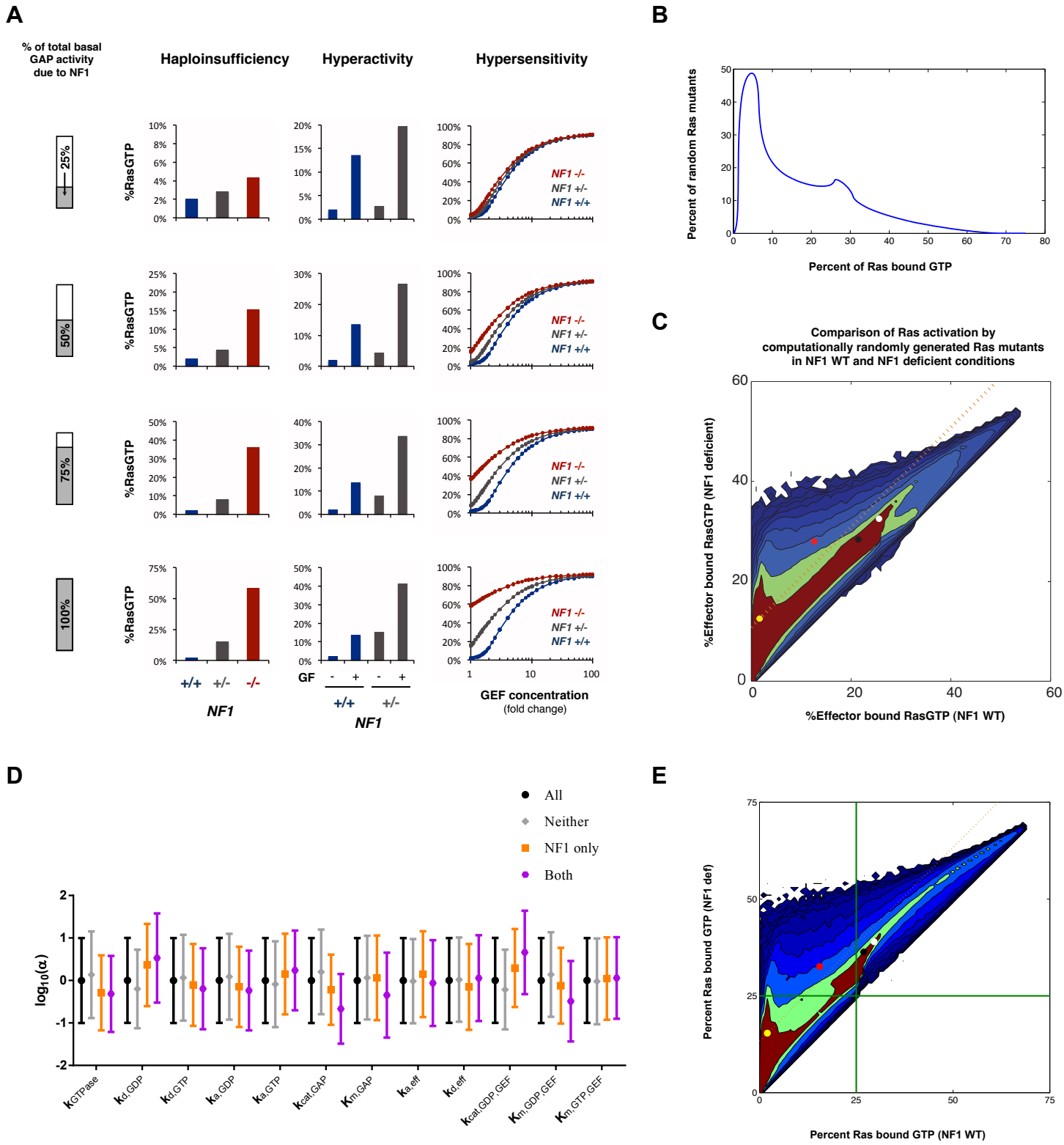
A
% of total basal GAP activity due to NF1
Haploinsufficiency
Hyperactivity
Hypersensitivity
25%
50%
75%
100%
%RasGTP
NF1 -/-
NF1 +/-
NF1 +/+
+/+ +/- -/-
NF1
GF - + - +
+/+ +/-
NF1
GEF concentration
(fold change)
B
Percent of random Ras mutants
Percent of Ras bound GTP
C
Comparison of Ras activation by computationally randomly generated Ras mutants in NF1 WT and NF1 deficient conditions
%Effector bound RasGTP (NF1 deficient)
%Effector bound RasGTP (NF1 WT)
D
All
Neither
NF1 only
Both
log10(α)
kGTPase
kd,GDP
kd,GTP
ka,GDP
ka,GTP
kcat,GAP
Km,GAP
ka,eff
kd,eff
kcat,GDP,GEF
Km,GDP,GEF
Km,GTP,GEF
E
Percent Ras bound GTP (NF1 def)
Percent Ras bound GTP (NF1 WT)

Figure S1

Figure S1, related to Figure 1. The Ras model predicts NF1 deficient phenotypes robustly.

(**A**) The model reproduces common NF1-deficient phenotypes, and shows robustness under different levels of GAP deficiency. We investigated the model's ability to reproduce three phenotypes that are common to NF1-deficient systems: (1) *haploinsufficiency*, i.e. the partial increase in Ras signal when one copy of NF1 is lost; (2) *hyperactivity*, i.e. an increased signal amplitude in response to growth factor stimulation for NF1 deficient conditions compared to WT conditions; and (3) *hypersensitivity*, i.e. a heightened response to a lower concentration of growth factor in the NF1 deficient state. We further considered this for different proportions of GAP-activity due to NF1 (25%, 50%, 75%, and 100%, as indicted above, to the left of each row).

(**B**) The percentage of the one million computational random Ras mutants that exceeded this level of RasGTP in NF1-deficient conditions, but not in wild-type conditions.

(**C**) An alternative measure of Ras activation also demonstrates that NF1-deficient conditions can potentiate the effects of some Ras mutants. Similar to Figure 1C, but with the percentage of Ras effector proteins bound to RasGTP used as a measure of Ras activation. White, G12V; Black; G12D; Red, F28L; Yellow, WT Ras only.

(**D**) Summary statistics of the computational random mutants for key subsets. Each of the computational random mutants is specified by twelve independent parameters, each of which is specified as a multiple of the wild-type parameter value (e.g. $k_{GTPase,G12D} = \alpha\, k_{GTPase,WT}$). For each of the twelve independent parameters of a modeled computational random mutant, the average values of $x = \log_{10}(\alpha)$ and the standard deviation for: all computational random mutants ("All", black), computational random mutants where there was less than 25% total RasGTP for both WT and NF1 deficient contexts ("Neither", gray), computational random mutants where there was 25% or more total RasGTP in the NF1 deficient context but not in the wild-type context ("NF1 only", orange), or computational random mutants that resulted in 25% or more RasGTP in both wild-type and NF1 deficient conditions ("Both", violet).

(**E**) Modeling a NF1 point mutation produces similar results as a mutation resulting in loss of NF1 GAP expression. NF1 deficiency modeled in Figure 1 was for complete loss of GAP activity, such as by a NF1 gene deletion or a nonsense mutation resulting in a premature stop codon before the GAP domain. The effects of a NF1 point mutation were modeled by incorporating previous experimental data for the k_{cat} and K_m of a GAP domain mutation R1276A. White, G12V; Black; G12D; Red, F28L; Yellow, WT Ras only.

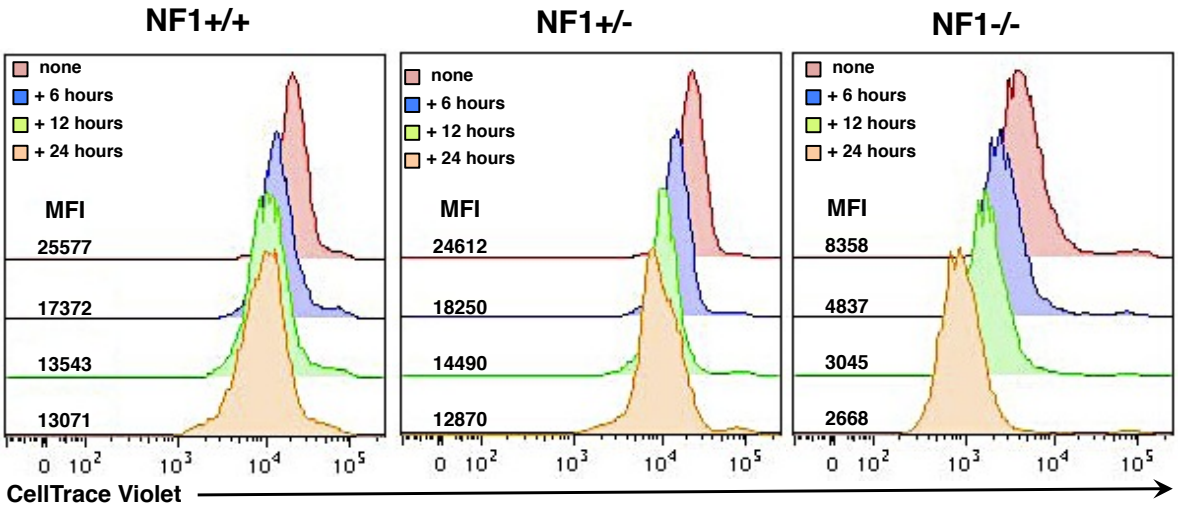
NF1+/+
NF1+/-
NF1-/-
none
+ 6 hours
+ 12 hours
+ 24 hours
MFI
25577
17372
13543
13071
24612
18250
14490
12870
8358
4837
3045
2668
0 10^2 10^3 10^4 10^5
CellTrace Violet

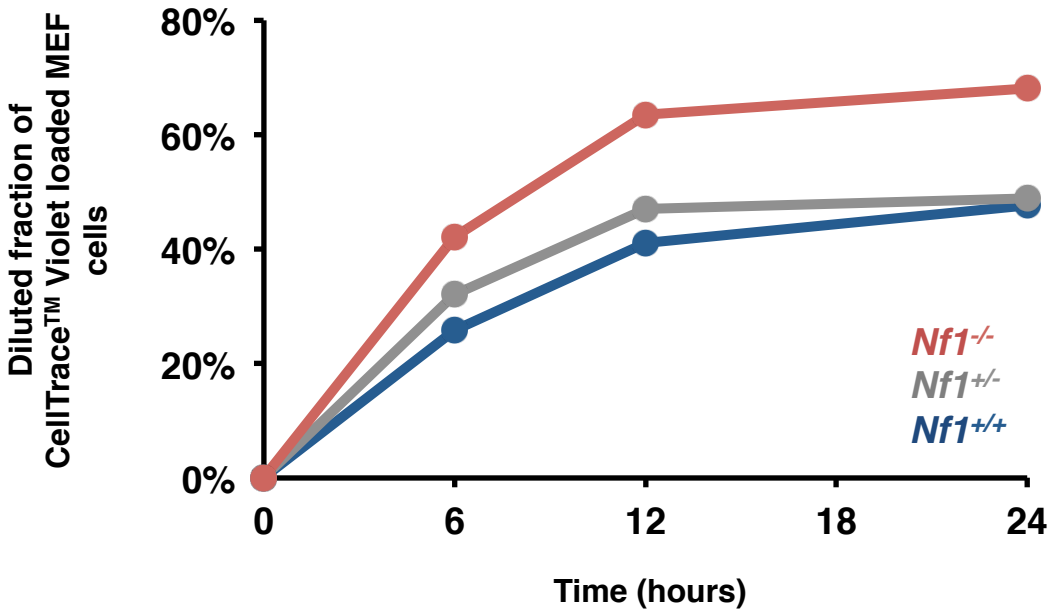
Diluted fraction of CellTrace™ Violet loaded MEF cells
80%
60%
40%
20%
0%
0
6
12
18
24
Time (hours)
Nf1-/-
Nf1+/-
Nf1+/+

Figure S2

Figure S2, related to Figure 2. Comparison of proliferation by MEFs with varying levels of neurofibromin expression.

(above) Proliferation assay for Nf1+/+, Nf1+/-, and Nf1-/- MEFs. (below) Analysis of the data from above to quantify the diluted fraction of the CellTrace Violet dye.

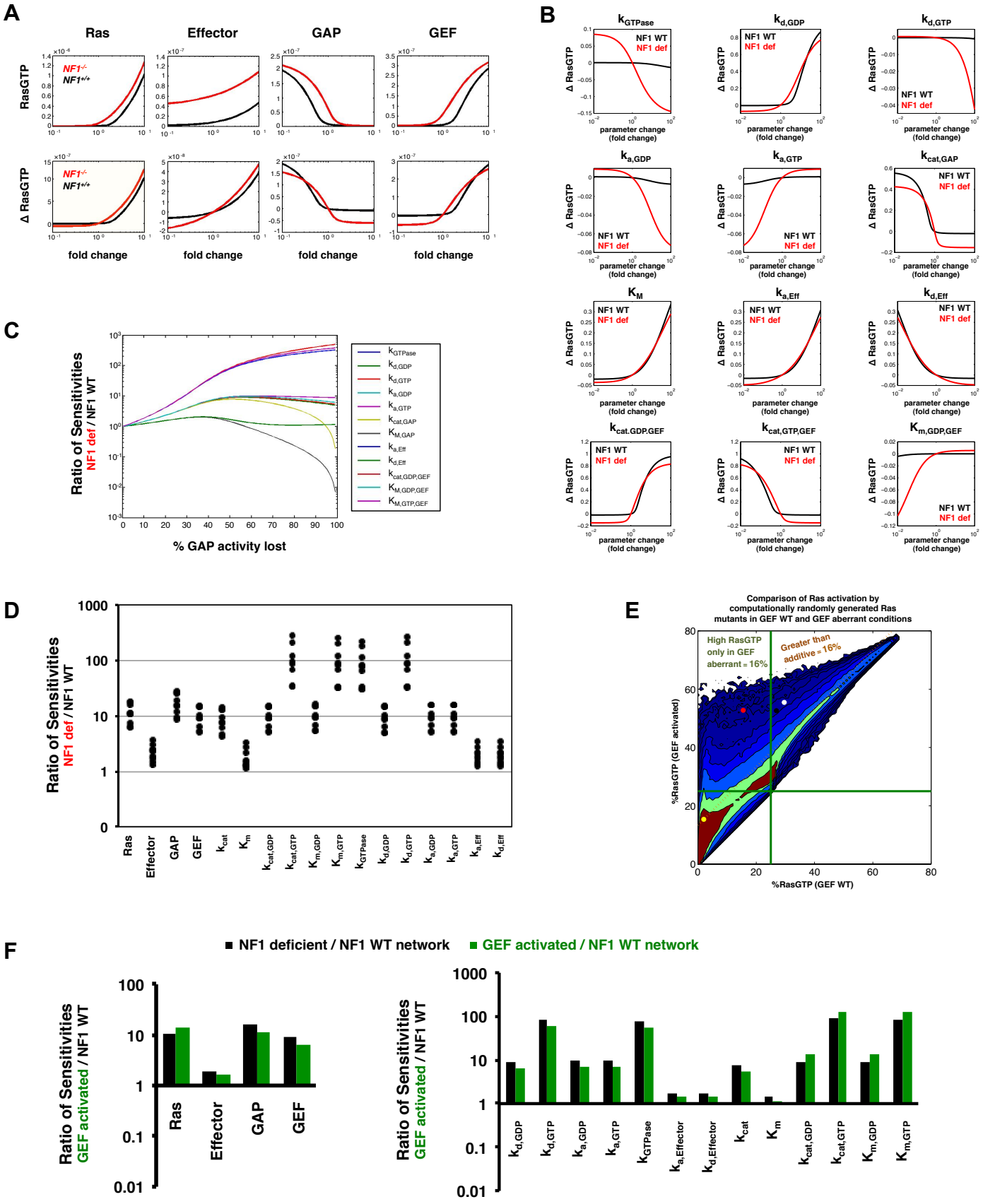
A
Ras
Effector
GAP
GEF
RasGTP
Δ RasGTP
NF1-/-
NF1+/+
fold change
B
kGTPase
kd,GDP
kd,GTP
ka,GDP
ka,GTP
kcat,GAP
KM
ka,Eff
kd,Eff
kcat.GDP,GEF
kcat,GTP,GEF
Km,GDP,GEF
NF1 WT
NF1 def
Δ RasGTP
parameter change (fold change)
C
Ratio of Sensitivities
NF1 def / NF1 WT
% GAP activity lost
kGTPase
kd,GDP
kd,GTP
ka,GDP
ka,GTP
kcat,GAP
KM,GAP
ka,Eff
kd,Eff
kcat,GDP,GEF
KM,GDP,GEF
KM,GTP,GEF
D
Ratio of Sensitivities
NF1 def / NF1 WT
Ras
Effector
GAP
GEF
kcat
Km
kcat,GDP
kcat,GTP
Km,GDP
Km,GTP
kGTPase
kd,GDP
kd,GTP
ka,GDP
ka,GTP
ka,Eff
kd,Eff
E
Comparison of Ras activation by computationally randomly generated Ras mutants in GEF WT and GEF aberrant conditions
High RasGTP only in GEF aberrant = 16%
Greater than additive = 16%
%RasGTP (GEF activated)
%RasGTP (GEF WT)
F
NF1 deficient / NF1 WT network
GEF activated / NF1 WT network
Ratio of Sensitivities
GEF activated / NF1 WT
Ras
Effector
GAP
GEF
kd,GDP
kd,GTP
ka,GDP
ka,GTP
kGTPase
ka,Effector
kd,Effector
kcat
Km
kcat,GDP
kcat,GTP
Km,GDP
Km,GTP

Figure S3

Figure S3, related to Figure 3. The Ras model predicts the acquisition of a state with increased sensitivity to perturbation robustly.

(**A**) Net change in RasGTP for a change in the indicated Ras network concentration parameter. RasGTP levels (M) and net changes in RasGTP levels are determined through model simulations when concentration parameters are varied in WT and NF1-deficient networks. Parameters are varied in terms of fold change from the baseline value of the parameter.

(**B**) Net changes in RasGTP for a change in the indicated Ras network reaction parameter. Net changes in RasGTP levels determined through model simulations when the reaction parameters are varied in NF1-WT and NF1-deficient networks. Parameters are varied in terms of fold change from the baseline value of the parameter. ΔRasGTP levels are normalized to the total amount of Ras.

(**C**) The proportion of total basal GAP activity lost influences the magnitude and sensitivity of the GAP-deficient network. The ratio of sensitivities (i.e. the change in RasGTP for a small change in each parameter) between GAP-deficient (e.g. NF1-deficient) and GAP-WT networks was determined for varying levels of basal GAP activity lost.

(**D**) The model-based predictions that NF1-deficient networks are more sensitive to perturbation are robust to changes in the basal protein concentrations. Nine concentration sets, which were previously used to assess the robustness of the Ras network model to the changes in specific concentrations of network proteins (Stites et al., 2007), were used here to assess predictions about neurofibromin deficiency. The same nine concentration sets were applied to the analysis presented in Fig. 3D. Each data point represents the ratio of sensitivities between NF1-deficient and NF1-WT networks for the specified parameter for one of the nine concentration sets.

(**E**) Ras GEF activation can potentiate the effects of a noncanonical Ras mutant. The same one million random mutants simulated and presented in Figure 1 for WT and NF1 deficient conditions were also simulated in the GEF activated states. Resulting levels of RasGTP are plotted for both WT and GEF activated conditions. White, G12V; Black; G12D; Red, F28L; Yellow, WT Ras only.

(**F**) Ras networks with increased basal GEF activity are more sensitive to perturbation. Calculations of the sensitivity of RasGTP levels to changes in model parameters were performed for networks with increased basal GEF activity and compared to the wild-type network, similar to what was done in Fig. 3D for neurofibromin deficiency. The ratio of sensitivities between the GEF activated and the NF1-WT network is presented (green). The ratio of sensitivities between the NF1-deficient network and the NF1-WT network is reproduced here for comparison (black).

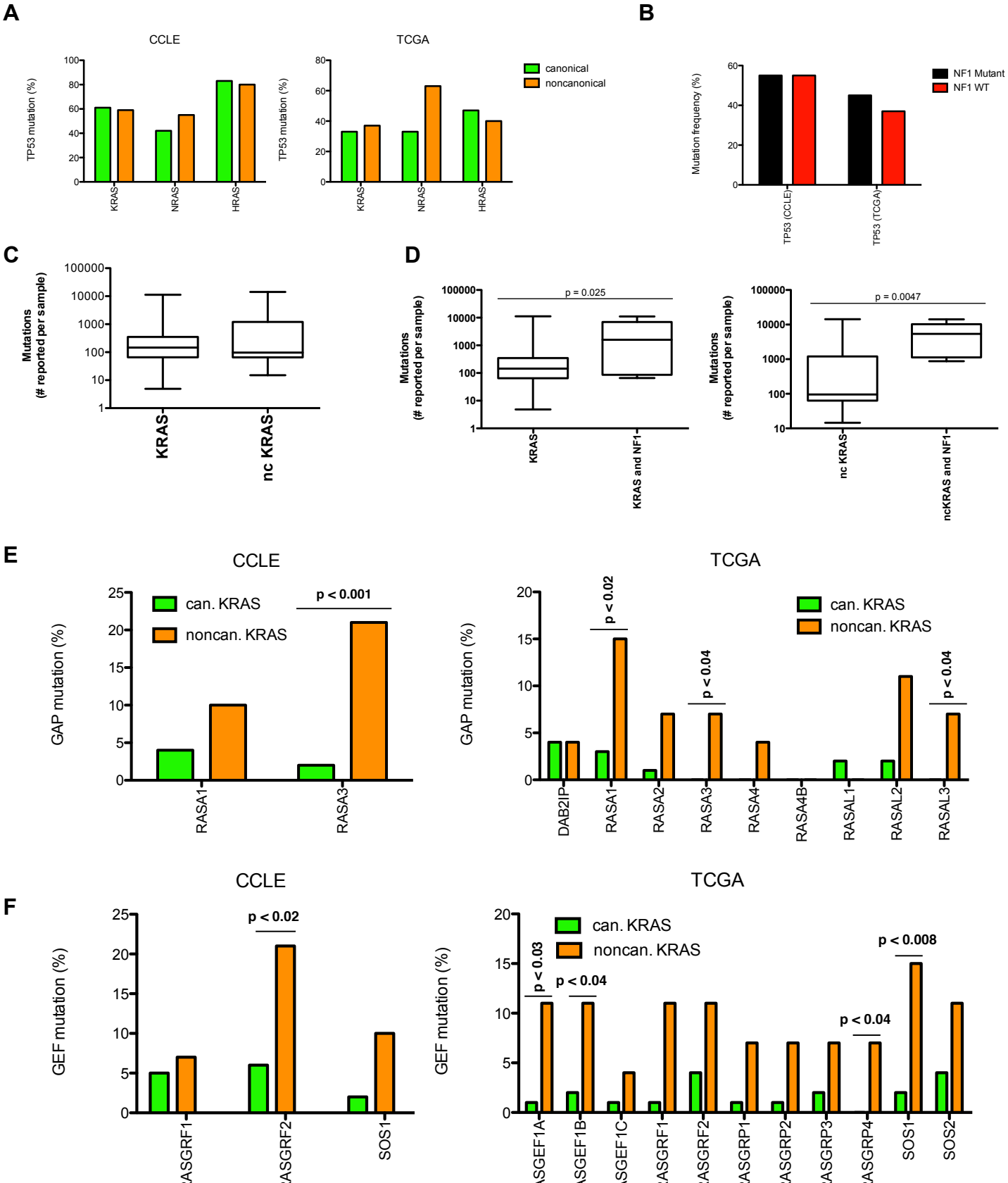
A
CCLE
TCGA
TP53 mutation (%)
canonical
noncanonical
KRAS
NRAS
HRAS
B
Mutation frequency (%)
NF1 Mutant
NF1 WT
TP53 (CCLE)
TP53 (TCGA)
C
Mutations (# reported per sample)
KRAS
nc KRAS
D
p = 0.025
p = 0.0047
KRAS and NF1
nc KRAS and NF1
E
CCLE
TCGA
GAP mutation (%)
can. KRAS
noncan. KRAS
p < 0.001
p < 0.02
p < 0.04
RASA1
RASA3
DAB2IP
RASA2
RASA4
RASA4B
RASAL1
RASAL2
RASAL3
F
GEF mutation (%)
p < 0.02
p < 0.03
p < 0.008
RASGRF1
RASGRF2
SOS1
RASGEF1A
RASGEF1B
RASGEF1C
RASGRP1
RASGRP2
RASGRP3
RASGRP4
SOS2

Figure S4

Figure S4, related to Figure 4. Analysis of cancer genome data sets finds an increased rate of co-occurrence for mutations within the Ras signaling network.

(**A**) Percentage of canonical and noncanonical RAS mutants that co-occur with a TP53 mutation within the CCLE dataset (left), or within the TCGA dataset (right). Differences are not significant by Fisher's exact test.

(**B**) The percentage of samples or without an NF1 that co-occur with a TP53 mutation was found for subsets of the CCLE and TCGA datasets. Differences are not significant by Fisher's exact test.

(**C**) The number of mutations per sample with canonical and noncanonical KRAS mutations. Data are from the TCGA. Differences were not significant by the Mann-Whiney test.

(**D**) There is an increased number of mutations per sample within samples found to have a combination of KRAS mutations and NF1 mutations. For the TCGA dataset, the number of mutations per sample was found for samples with a canonical KRAS mutation but no NF1 mutation and for samples with both canonical KRAS and NF1 mutations (left). The number of mutations per sample was also found for samples with a noncanonical KRAS mutation but no NF1 mutation and for samples with both noncanonical KRAS and NF1 mutation (right). The increase was statistically significant for canonical KRAS and NF1 mutations ($p = 0.025$) and for noncanonical KRAS and NF1 mutations ($p = 0.0047$) by the Mann-Whitney test.

(**E**) Co-occurrence of noncanonical Ras mutants with NF1 and Ras GAP mutants. The percentage of canonical and noncanonical KRAS mutants that co-occur with a Ras GAP mutation within the CCLE dataset (above) or within the TCGA dataset (below). The p-value for all panels is by Fisher's exact test.

(**F**) Co-occurrence of noncanonical Ras mutants with Ras GEF mutants. The percentage of canonical and noncanonical KRAS mutants that co-occur with a Ras GEF mutation within the CCLE dataset (above) or within the TCGA dataset (below). The p-value for all panels is by Fisher's exact test.

Supplemental Methods

Modeling the Ras signaling network

We have previously developed a mathematical model of the processes that regulate which nucleotide is bound to the Ras GTPases (Figure 3A). Model predictions for quantities, such as the amount of RasGTP present when different Ras mutants are transfected into a cell line, have previously been shown to compare well with experimentally determined values. We previously used this model to study the constitutively elevated levels of Ras pathway signals that are produced by canonical oncogenic Ras mutants (Stites et al., 2007). Among the predictions of our earlier model was that oncogenic Ras mutants lead to increased activation of wild-type Ras within the same cell. The different roles of wild-type and oncogenic mutant Ras in cancer have since become an important topic in cancer biology (Grabocka et al., 2014; Jeng et al., 2012; Lim et al., 2008; Young et al., 2013). Additionally, although the k_{cat} for the GAP activity on RasGTP is approximately ten-thousand times greater than the rate constant for spontaneous GTPase activity, the model predicted that a GAP-insensitive mutant with wild-type-level GTPase activity would be much less active than a mutant that was both GAP-insensitive and GTPase impaired (like the canonical Ras mutants). After our predictions were made, a GAP-insensitive mutant with GTPase activity near wild-type levels was reported to have been found in a Noonan syndrome patient, and, consistent with our model's predictions and contrary to conventional wisdom, levels of RasGTP for this mutant were significantly less than the canonical Ras mutants (Schubbert et al., 2007).

We have used modeled levels of RasGTP and levels of effector bound to RasGTP as measures of Ras activation. We here focus on levels of RasGTP as a computational readout as it tends to be an intuitive measure of Ras signaling and therefore facilitates communication. Levels of RasGTP can be measured by thin-layer chromatography (Boykevisch et al., 2006; Gibbs et al., 1990), and can be measured after RasGTP specific binding and pull-down with constructs of the Raf-1 Ras binding domain (RBD) (Courtois-Cox et al., 2006; Shapira et al., 2007). The level of effector bound to RasGTP is less easily measured directly, in part because of the large number of proteins with a Ras binding domain that bind to the Ras proteins (Rodriguez-Viciana et al., 2004). Antibodies and methods for measuring ERK phosphorylation by flow-

cytometry are particularly well validated and are a common and well-established surrogate measure of Ras pathway activation (Trampont et al., 2010). The activation of effectors directly downstream of Ras, such as Raf, involves multiple processes other than simply binding to Ras (Hu et al., 2013). Measurements of signaling below Raf (such as ERK phosphorylation) can indicate that Ras signals have been transmitted beyond the binding of Ras to Raf. We therefore use flow-cytometry measurements of ERK phosphorylation to measure Ras activation because this is a well-accepted measure of Ras activation, because the reagents and methods are well established, and because single-cell measurements of ERK phosphorylation allow us to measure how changes in expression reflect changes in Ras activation.

Modeling GAP deficiency

When we originally developed our Ras model, we focused upon neurofibromin as the basally active Ras GAP that maintains low-levels of Ras signal in non-stimulated cells (Ahmadian et al., 1997). Of all Ras GAPs, neurofibromin has the best evidence for contributing to the basal regulation of steady-state RasGTP levels and the clearest association with cancer. *NF1*, the gene coding for neurofibromin, is one of the most commonly mutated genes in lung cancer (Ding et al., 2008), ovarian cancer (Kan et al., 2010; The Cancer Genome Atlas Netwrok, 2011), and glioblastoma (Brennan et al., 2013; Parsons et al., 2008; The Cancer Genome Atlas Network, 2008). Loss of a single copy of tumor suppressor gene *NF1* does not appear capable of promoting cancer alone, although *NF1* displays haploinsufficiency and a loss of one functional allele is sufficient to cause a small increase in RasGTP and the cellular proliferation rate (Shapira et al., 2007). Individuals with neurofibromatosis also have an increased risk of developing many different tumors (Williams et al., 2009). The disease neurofibromatosis is caused by germline loss of one functional copy of *NF1*, which further highlights that a small, partial increase in Ras signal can have pathological consequences.

Loss of the full complement of neurofibromin can induce negative feedback to counteract the resultant increase in Ras pathway activation (Courtois-Cox et al., 2006). However, there is abundant evidence that negative feedback is not sufficient to counteract the consequences of decreased GAP activity. Neurofibromin deficient cells display elevated levels of RasGTP (Bollag et al., 1996), ERK phosphorylation (Shapira et al., 2007), and proliferation (Joseph et al., 2008). Indeed, the disease

neurofibromatosis highlights that negative feedback is not sufficient to completely counteract loss of neurofibromin (Williams et al., 2009).

Pathological *NF1* mutations, such as those associated with cancer and neurofibromatosis, commonly result in loss of expression of neurofibromin (The Cancer Genome Atlas Network, 2008). Gene mutations within the Ras pathway can also result in a protein product with altered biochemistry. For example, the oncogenic Ras mutant RasG12V has an apparent complete loss of k_{cat} for GAP activity on Ras, an order of magnitude decrease in its intrinsic GTPase reaction, slight variations in nucleotide affinity, and slightly increased affinity for its effector Raf. Such changes can be applied to the model to make predictions that match well with experimental data (Stites et al., 2007). Thus, mathematical models can find behaviors that naturally emerge from the changes in rate constants and concentrations that follow from gene mutation, and in that manner predict how the system responds to particular mutations (Stites and Ravichandran, 2012).

In the case where all basal GAP activity is due to NF1, complete loss of both copies of NF1 would result in zero basal GAP activity and loss of one copy would result in a 50% reduction in GAP concentration (if there is no feedback changes in expression). However, although we have focused on neurofibromin as the basally active Ras GAP, other Ras GAPs may also serve to maintain low levels of Ras signaling in non-stimulated conditions. For example, DAB2IP has been shown to serve the role of a basally active Ras GAP in prostate cancer cells (Min et al., 2010). In a situation where DAB2IP and NF1 equally contribute to basal GAP activity, a homozygous loss of NF1 might result in a 50% reduction in basal GAP concentration. As our model more generally describes the behavior of basally active Ras GAPs on regulating Ras pathway activation, our model analysis should more generally apply to conditions where other Ras GAPs serve the role of basally active Ras GAP. In cases where more than one Ras GAP contributes to basal Ras activation, loss of NF1 (or loss of another Ras GAP) could result in a fraction other than 50% of total, basal, Ras GAP activity being lost. We considered fractions from 0% to 100% of total, basal, Ras GAP activity being lost and found that our model predictions were robust to the level of GAP deficiency modeled (Figure S3C). As we are using the model to gain non-obvious insights into the consequences of NF1/GAP deficiency and to the consequences of combinations of

mutations that can then be tested experimentally and/or bioinformatically, we use a 50% reduction in NF1 as a convenient starting point.

We wished to determine if the model could apply to a NF1 deficient system with additional perturbations. Three behaviors common to NF1 deficient networks were considered to evaluate the predictive ability of the model in NF1 deficient conditions: haploinsufficiency, i.e. the partial increase in Ras signal when one copy of *NF1* is lost (Bennett et al., 2003; Shapira et al., 2007; Yang et al., 2006a); hyperactivity, i.e. an increased signal amplitude in response to growth factor stimulation for NF1 deficient conditions compared to WT conditions (Ingram et al., 2000; Yang et al., 2006a; Yang et al., 2006b); and hypersensitivity, i.e. the response to a lower concentration of growth factor in NF1 deficient cells such that a growth factor dose response curve is left-shifted (Bennett et al., 2003; Bollag et al., 1996; Yang et al., 2006a; Yang et al., 2006b). The model was able to reproduce all of these key features of NF1 signaling (Figure S1A). Only the GAP levels were varied to reflect NF1 deficiency, only the GEF levels were varied to reflect growth factor stimulation, and we did not have to tune or otherwise adjust our model for it to produce all three behaviors. We considered different levels of GAP loss to investigate how the proportion of total, modeled, basal GAP activity removed would impact the predictive ability of the model. We removed 50% of total basal GAP activity to model the NF1-/- state, removed 25% to represent the NF1+/- state, and removed 0% (i.e. no removal) for the NF1+/+ (WT) state. We observed haploinsufficiency, hyperactivity, and hypersensitivity for this wide range of NF1 contributions to basal GAP activity (Figure S1A).

The above approach for modeling neurofibromin deficiency should apply well to mutations that result in loss of expression of neurofibromin (such as gene/chromosome deletions) and to mutations that result in the expression of a neurofibromin protein that does not include the GAP domain (such as may occur with a nonsense mutation that results in a stop codon prior to the GAP domain). *NF1* mutations may also result in nonsense mutations that express full-length protein but with altered biochemistry. Mutations to the GAP-related domain, for example, may result in altered k_{cat} and K_m for the GAP activity on Ras. We also modeled the behavior of NF1 point mutations by modeling the NF1 R1276A mutant. Sermon et al previously measured a k_{cat} of 0.02/s for R1276A compared to a k_{cat} of 23/s for wild-type neurofibromin, and no change in the interaction with Ras, suggesting no change to K_m (Sermon et al., 1998). The change in

k_{cat} was applied to the modeled NF1 mutant. We considered 50% of total GAP to be mutant and 50% of total GAP to be wild-type (Figure S1E).

Computational Random Mutagenesis

Within a model with all wild-type Ras, the parameters of the model correspond to observable biochemical properties of wild-type Ras protein. For example, the rate constant for the intrinsic GTPase activity of Ras is a value of the rate constant measured experimentally for wild-type Ras (Donovan et al., 2002). The network containing a Ras mutant can be modeled by using the parameters appropriate for a Ras mutant. For example, RasG12D is known to have a reduced rate of the intrinsic GTPase activity (Eccleston et al., 1991). Applying all known changes to the parameters governing the known reactions involving Ras allows the mutant to be modeled. It is possible to specify the rate constant for a mutant as a multiple of the wild-type parameter. For example, the rate constant for the intrinsic GTPase activity of RasG12D (k,GTPase,G12D) can be specified as

$k_{,GTPase,G12D} = \alpha\ k_{,GTPase,WT}$

where here

$\alpha = k_{GTPase,G12D} / k_{GTPase,WT}$.

This approach of specifying mutant parameters as a multiple of the wild-type parameter is useful for specifying computational random mutants.

Computational random Ras mutants were generated by obtaining a random set of factors (α_i with i=1:12) with which to vary each of the twelve independent RasWT reaction parameters. Each random mutant was generated by first creating a set of twelve random numbers from a random number distribution with a mean of zero and standard deviation of 1 (x_i with i=1:12). This random number, x_i, was transformed into the corresponding parameter multiplication factor, $\alpha_i=10^x$. These were then applied to twelve free reaction parameters ($k_{mut,i} = \alpha_i\ k_{WT,i}$). The remaining parameter, ($k_{catGTPGEF}$) was calculated from the other parameters to ensure thermodynamically consistent parameters for nucleotide exchange (whether GEF-mediated or free nucleotide exchange). Each random mutant was specified by these new parameters. The model was then simulated with 25% of total Ras comprised of the computational random mutant and the remaining 75% of total Ras comprised of wild-type Ras. Simulations

were run until steady-state was reached, and levels of RasGTP and RasGTP-effector complex were saved. This was done for all one million computational random mutants.

Sensitivity Analyses

Sensitivity analysis, or the process of determining how model outputs vary in response to changes in model parameters, has long been a part of the analysis of mathematical models of cell signaling networks (Kitano, 2002; Schoeberl et al., 2002). There are many potential uses for a sensitivity analysis (Zi, 2011), including the study of how network behavior might depend on variations within the underlying network (Gaudet et al., 2012) and where mutations in the network might have the largest effect (Chen et al., 2014). More generally, the results of a sensitivity analysis can help reveal behaviors of the studied network that were not obvious by prior inspection and are interesting candidates for further computational and/or experimental study (Benedict et al., 2011).

The Ras model studied here was developed so that the parameters of the model corresponded directly to observable biochemical properties. The output of the model studied, levels of RasGTP, corresponds to a biologically important observable. Increased levels of RasGTP are believed to be an important part of pro-cancer signaling. Our analysis of changes to which model parameters (biochemical properties) are likely to result in large changes in RasGTP levels therefore seems useful for identifying properties that could result in increased pro-cancer signaling. As the total amount of Ras pathway signal appears to be an important factor in the cellular phenotype of neurofibromin deficient cells (Shapira et al., 2007) and in cells containing Ras mutants (Donovan et al., 2002), we focus our sensitivity on the net total change in Ras GTP for a change in a parameter. The change in RasGTP for a change in a model parameter was determined with simulations and/or with analytical calculations. For simulations, a single parameter was adjusted by ±0.1% of its value in the WT network, and the resultant level of RasGTP was determined with model simulations. The difference in RasGTP, or ΔRasGTP, was determined from the two resulting levels of steady-state RasGTP. This was done for WT and NF1/GAP-deficient networks. The ratio of ΔRasGTP for the NF1-deficient network to ΔRasGTP for the WT network was used as a measure of relative sensitivity to a change in a single parameter value.

Analytical calculations were performed using the same set of reactions and conservation laws for total Ras and total effector. These reaction equations were algebraically reduced to an expression that relates the levels of RasGTP to each parameter. Further algebraic manipulation reduced these equations to a single expression that implicitly relates steady-state levels of RasGTP to each parameter, G(RasGTP,k)=0, where k indicates all of the parameters of the model (including concentrations, rate constants, and enzymatic parameters. To determine $\frac{\partial\, Total\ RasGTP}{\partial\, parameter}$ for each parameter, we use the implicit function theorem, with

$$\frac{\partial\, Total\ RasGTP}{\partial\, parameter} = -\frac{\partial G/\partial parameter}{\partial G/\partial RasGTP}$$

The resulting expression was then numerically evaluated at the steady-state level of RasGTP with the model parameter values. This was done for WT (100% basal GAP present) and NF1-deficient (50% basal GAP present) conditions. The ratio of $\frac{\partial\, Total\ RasGTP}{\partial\, parameter}$ for the NF1-deficient network to the $\frac{\partial\, Total\ RasGTP}{\partial\, parameter}$ for the WT network was used as a measure of relative sensitivity to a change in a single parameter value, just as when these changes were determined with simulations. The values of the slopes determined from this analytic approach were compared to values derived from numerical simulations to verify the accuracy of the algebraic and numeric evaluation. The use of two separate approaches to yield the same results helps assure the validity of the modeling results (Gunawardena, 2014).

We note that we focus here on the absolute increase in RasGTP from the respective NF1-WT and NF1-deficient conditions rather than the relative change in RasGTP because it appears that the total amount of Ras pathway activation, and not the relative change from each mutation, represents an important feature in cancer cell signaling (Donovan et al., 2002; Shapira et al., 2007). We also noted that the increased magnitude change in RasGTP does not occur for some large changes to reaction rate constants (Figures S3A,B for several parameters). This is likely because the NF1-deficient network has a higher proportion of total Ras in the RasGTP form, and a smaller net change is needed to reach saturation in RasGTP levels. However, the level of constitutive Ras pathway signaling associated with disease causing mutations appears to be far less than saturating (Donovan et al., 2002). Thus, the increased magnitude change within NF1-deficient conditions that occurs from an already elevated baseline appears relevant to cancer progression.

Modeling GEF activation

Mutations to the Ras GEF Sos1 have been found in Noonan syndrome and have been found to result in modest increases in RasGTP levels (Tartaglia et al., 2007). The amount of basal GEF activity on Ras could also be increased by an increase in upstream signaling (e.g. increased basal EGFR signaling leading to increased basal Sos1 recruitment to the membrane). We considered whether increased levels of basal GEF activity might also influence the effects of noncanonical Ras mutations. To investigate this, we used our mathematical model to simulate the same set of one million computational random Ras mutants within the condition of a partial increase in GEF activity. Partial GEF activation could also increase the effects of some Ras mutants (Figure S3E). We note that the effects of a GEF mutation or an upstream mutation that results in increased GEF activation would likely have wide range of potential levels of GEF (and resultant Ras) activation. To facilitate comparisons between aberrant GEF conditions with GAP-deficient conditions, we wanted to have a similar baseline of RasGTP activity for the two conditions. We therefore chose to model aberrant GEF activity by using an elevated level of basally active Ras GEF that would result in the same level of basal RasGTP as would result from a modeled 50% decrease in the basal GAP concentration. A 2.0865× increase in the modeled concentration of basal GEF activity resulted in 15.38% of Ras being bound to GTP, and a decrease of 50% of the modeled concentration of basal GAP also resulted in 15.38% of Ras being bound to GTP.

Our computational random mutagenesis found that a modest increase in basal GEF activity could also potentiate the effects of some (but not all) Ras mutants. The proportion of Ras mutants that were strongly activating in GEF aberrant conditions but not in WT conditions (16% of simulated mutants) was similar to that observed for GAP deficiency (15% of simulated mutants). The fraction of mutants that displayed greater than additive behavior with aberrant GEF signaling (16%) was also similar to what was observed for GAP deficiency (13%). Overall, these simulations suggest that mutations that result in increased levels of basal GEF activation may potentiate Ras mutant signals, essentially similar to mutations in NF1 and other Ras GAP proteins.

Cell transfection

Immortalized Nf1+/+, Nf1+/-, and Nf1-/- MEF cells were obtained from Dr. Reuven Stein at the George S. Wise Faculty of Life Sciences, Tel Aviv, Israel. Cells were maintained as described previously (Shapira et al., 2007). The plasmid encoding 3xHA-tagged H RasWT was obtained from Missouri S&T cDNA Resource Center. Ras mutants H RasG12D and H RasF28L were generated using the QuikChange mutagenesis kit (Stratagene) and confirmed by sequencing. V5 tagged NF1-GRD was provided by Dr. David Largaespada at the University of Minnesota, Minneapolis, MN. MEF cells were plated on six-well plates and transiently transfected with 3µg of plasmid constructs using Lipofectamine 2000 and according to manufacturer's instructions (Invitrogen). After 4 hours, fresh growth medium was added for 6 hours. Cells were starved for 12 hours in DMEM 0.5% fetal calf serum (FCS) and then harvested for cytometry analysis.

Immunoblotting

MEF cells were subjected to lysis in a buffer containing 50 mM Tris (pH 7.6), 150 mM NaCl, 1 mM EDTA, 1% Triton X-100 10 mM sodium pyrophosphate, 10 mM sodium fluoride, 1 mM sodium orthovanadate, and protease inhibitors (Calbiochem). Total cell lysates were separated by 5-20% gradient SDS-PAGE and transferred to PVDF membrane. Membranes were blocked with 5% milk in 1% tween-20 Tris-buffered saline buffer. Proteins were detected by antibodies against NF1 (Upstate Biotechnology, Millipore), Erk1/2 (Cell signaling Tech), phospho-Erk1/2 (Cell Signaling Tech), HA-tag (Cell Signaling Tech), V5-tag (Millipore), p120 RasGAP (BD biosciences). Immunoblots were developed using enhanced chemiluminescence (Pierce, Rockford, IL).

Quantitative PCR

Total RNAs were extracted from MEF cells with a QIAshredder and RNeasy kit (Qiagen). The SuperScript III kit (Invitrogen) was used for reverse transcription. TaqMan Gene Expression assays for Rasa1, Rasa4, DAB2IP, and Nf1 (Applied Biosystems) were used for quantitative PCR. Samples were amplified in duplicate and target transcripts were normalized to Hprt1 mRNA as a housekeeping gene. The relative expression of each target gene was calculated by the comparative cycling method with

StepOne v2.1 software (Applied Biosystems). The standard deviation was calculated after normalization of multiple experiments.

Flow cytometry

MEF cell staining for phospho-Erk1/2 (referred to as phoshpo-ERK or pERK) and HA-tagged H-Ras was performed as described previously (Stites et al., 2007). Data were acquired on a FACS CantoII (Becton Dickinson). Stimulation of cells with PMA served as a positive control for maximal pERK activation. The inhibition of the pERK signal inhibitory ERK peptide and the U0126 drug served to confirm the veracity of the observed pERK signals in this flow cytometry based detection assay.

Cells were gated based on the intensity of the HA signal to define "high" and "low" HA expressing populations. The same intensity gates were used for comparisons between Nf1+/+ and Nf1-/- MEFs, as well as between cells transfected with different Ras constructs. Mean pERK intensity was quantified for high and low HA expression, and the ratio of differences between high and low HA expression,

$$ratio = \frac{HA_{high}(Nf1^{-/-}) - HA_{low}(Nf1^{-/-})}{HA_{high}(Nf1^{+/+}) - HA_{low}(Nf1^{+/+})}$$

was used as a measure of the change in sensitivity between Nf1-/- and Nf1+/+ conditions. To assess cell proliferation and allow cell cycle synchronization, MEF cells were starved for 12 hours in DMEM 0.5% FCS and stained with CellTrace™ Violet Cell proliferation kit, according to manufacturer's instructions. Stained cells were then harvested in a time course and their state of proliferation analyzed by cytometry.

Genomic Data Analysis

Investigations looking for an increased co-occurrence of uncommonly mutated genes require large datasets. We consider here two large datasets, the Cancer Cell Line Encyclopedia (Barretina et al., 2012), and the TCGA dataset of twelve types of cancers (Kandoth et al., 2013). Mutations for the genes of Ras network proteins (*ARAF*, *BRAF*, *DAB2IP*, *EGFR*, *HRAS*, *KRAS*, *NF1*, *NRAS*, *PIK3CA*, *RAF1*, *RALGDS*, *RASA1*, *RASA2*, *RASA3*, *RASA4*, *RASA4B*, *RASAL1*, *RASAL2*, *RASAL3*, *RASGEF1A*, *RASGEF1B*, *RASGEF1C*, *RASGRF1*, *RASGRF2*, *RASGRP1*, *RASGRP2*, *RASGRP3*, *RASGRP4*, *SOS1*, and *SOS2*) and for *TP53* were obtained from the CCLE portal

(http://www.broadinstitute.org/ccle) and/or from published cancer genome publications (Barretina et al., 2012; Kandoth et al., 2013). Exonic missense and nonsense mutation, and exonic insertions and deletions were considered.

We assess co-occurrence with Fisher's Exact Test, as has been the standard for genomic analyses looking for co-occurrence (Kandoth et al., 2013; Thomas et al., 2007; Yates and Campbell, 2012; Yeang et al., 2008). Coincident mutations were counted as the number of distinct samples with at least one mutation in the specified genes. For communicating different rates of co-occurrence between two genes (e.g. A and B), we may present the rate of a mutation to A when B is or is not mutated. We highlight that even though we are examining the same number of total cancer genomes for the different combinations of gene mutations, that the number of times a specific gene is found to be mutated can vary widely. Due to this variability, we present the percentage of the mutated gene of interest that co-occurs with another mutated gene (i.e. 10% of canonical *KRAS* mutations co-occur with an *NF1* mutation) to facilitate comparisons between members of a class of genes, and use the p-value from the Fisher's Exact test, which takes into account the exact number of mutations, genomes analyzed, and the various co-occurrences, to determine whether the pattern of co-occurrence is statistically significant. *TP53* mutations were included as a measure of the similarity between considered subsets of the CCLE and TCGA data. We used the HGMD database (Stenson et al., 2014) to identify which *NF1* mutations have previously been found in patients with neurofibromatosis.

That combinations of mutations within the Ras network may be capable of functional cooperation may seem to contrast with the conventional wisdom that mutations do not co-occur within the same pathway (Thomas et al., 2007; Yeang et al., 2008). However, conventional wisdom is based on the behavior of the strongly activating, canonical mutations, which do not co-occur. Indeed, our modeling suggests that combinations of mutations involving a strongly activating canonical mutation have a less-than-additive total response and would therefore not be expected to acquire a significant competitive advantage (Figure 1A). Therefore, our modeling is consistent with the lack of co-occurrence between strongly activating canonical mutations. Combinations of NF1 and BRAF V600E mutations have been observed in melanoma samples and cell lines, and mouse models that have been engineered to express BRAF V600E and to also have decreased Nf1 expression have demonstrated a cooperative effect for this combination (Maertens et al., 2013).

Supplementary References

Ahmadian, M. R., Hoffmann, U., Goody, R. S., and Wittinghofer, A. (1997). Individual rate constants for the interaction of Ras proteins with GTPase-activating proteins determined by fluorescence spectroscopy. Biochemistry *36*, 4535-4541.

Bennett, M. R., Rizvi, T. A., Karyala, S., McKinnon, R. D., and Ratner, N. (2003). Aberrant growth and differentiation of oligodendrocyte progenitors in neurofibromatosis type 1 mutants. J Neurosci *23*, 7207-7217.

Bollag, G., Clapp, D. W., Shih, S., Adler, F., Zhang, Y. Y., Thompson, P., Lange, B. J., Freedman, M. H., McCormick, F., Jacks, T., and Shannon, K. (1996). Loss of NF1 results in activation of the Ras signaling pathway and leads to aberrant growth in haematopoietic cells. Nat Genet *12*, 144-148.

Boykevisch, S., Zhao, C., Sondermann, H., Philippidou, P., Halegoua, S., Kuriyan, J., and Bar-Sagi, D. (2006). Regulation of ras signaling dynamics by Sos-mediated positive feedback. Curr Biol *16*, 2173-2179.

Brennan, C. W., Verhaak, R. G., McKenna, A., Campos, B., Noushmehr, H., Salama, S. R., Zheng, S., Chakravarty, D., Sanborn, J. Z., Berman, S. H.*, et al.* (2013). The somatic genomic landscape of glioblastoma. Cell *155*, 462-477.

Ding, L., Getz, G., Wheeler, D. A., Mardis, E. R., McLellan, M. D., Cibulskis, K., Sougnez, C., Greulich, H., Muzny, D. M., Morgan, M. B.*, et al.* (2008). Somatic mutations affect key pathways in lung adenocarcinoma. Nature *455*, 1069-1075.

Eccleston, J. F., Moore, K. J., Brownbridge, G. G., Webb, M. R., and Lowe, P. N. (1991). Fluorescence approaches to the study of the p21ras GTPase mechanism. Biochemical Society transactions *19*, 432-437.

Gibbs, J. B., Marshall, M. S., Scolnick, E. M., Dixon, R. A., and Vogel, U. S. (1990). Modulation of guanine nucleotides bound to Ras in NIH3T3 cells by oncogenes, growth factors, and the GTPase activating protein (GAP). J Biol Chem *265*, 20437-20442.

Grabocka, E., Pylayeva-Gupta, Y., Jones, M. J., Lubkov, V., Yemanaberhan, E., Taylor, L., Jeng, H. H., and Bar-Sagi, D. (2014). Wild-type h- and N-ras promote mutant k-ras-driven tumorigenesis by modulating the DNA damage response. Cancer Cell *25*, 243-256.

Gunawardena, J. (2014). Models in biology: 'accurate descriptions of our pathetic thinking'. BMC biology *12*, 29.

Hu, J., Stites, E. C., Yu, H., Germino, E. A., Meharena, H. S., Stork, P. J., Kornev, A. P., Taylor, S. S., and Shaw, A. S. (2013). Allosteric activation of functionally asymmetric RAF kinase dimers. Cell *154*, 1036-1046.

Ingram, D. A., Yang, F. C., Travers, J. B., Wenning, M. J., Hiatt, K., New, S., Hood, A., Shannon, K., Williams, D. A., and Clapp, D. W. (2000). Genetic and biochemical evidence that haploinsufficiency of the Nf1 tumor suppressor gene modulates melanocyte and mast cell fates in vivo. J Exp Med *191*, 181-188.

Jeng, H. H., Taylor, L. J., and Bar-Sagi, D. (2012). Sos-mediated cross-activation of wild-type Ras by oncogenic Ras is essential for tumorigenesis. Nat Commun *3*, 1168.

Joseph, N. M., Mosher, J. T., Buchstaller, J., Snider, P., McKeever, P. E., Lim, M., Conway, S. J., Parada, L. F., Zhu, Y., and Morrison, S. J. (2008). The loss of Nf1 transiently promotes self-renewal but not tumorigenesis by neural crest stem cells. Cancer Cell *13*, 129-140.

Kan, Z., Jaiswal, B. S., Stinson, J., Janakiraman, V., Bhatt, D., Stern, H. M., Yue, P., Haverty, P. M., Bourgon, R., Zheng, J.*, et al.* (2010). Diverse somatic mutation patterns and pathway alterations in human cancers. Nature *466*, 869-873.

Kitano, H. (2002). Computational systems biology. Nature *420*, 206-210.

Lim, K. H., Ancrile, B. B., Kashatus, D. F., and Counter, C. M. (2008). Tumour maintenance is mediated by eNOS. Nature *452*, 646-649.

Min, J., Zaslavsky, A., Fedele, G., McLaughlin, S. K., Reczek, E. E., De Raedt, T., Guney, I., Strochlic, D. E., Macconaill, L. E., Beroukhim, R.*, et al.* (2010). An oncogene-tumor suppressor cascade drives metastatic prostate cancer by coordinately activating Ras and nuclear factor-kappaB. Nat Med *16*, 286-294.

Parsons, D. W., Jones, S., Zhang, X., Lin, J. C., Leary, R. J., Angenendt, P., Mankoo, P., Carter, H., Siu, I. M., Gallia, G. L.*, et al.* (2008). An integrated genomic analysis of human glioblastoma multiforme. Science *321*, 1807-1812.

Rodriguez-Viciana, P., Sabatier, C., and McCormick, F. (2004). Signaling specificity by Ras family GTPases is determined by the full spectrum of effectors they regulate. Mol Cell Biol *24*, 4943-4954.

Schubbert, S., Zenker, M., Rowe, S. L., Boll, S., Klein, C., Bollag, G., van der Burgt, I., Musante, L., Kalscheuer, V., Wehner, L. E.*, et al.* (2006). Germline KRAS mutations cause Noonan syndrome. Nat Genet *38*, 331-336.

Smith, G., Bounds, R., Wolf, H., Steele, R. J., Carey, F. A., and Wolf, C. R. (2010). Activating K-Ras mutations outwith 'hotspot' codons in sporadic colorectal tumours - implications for personalised cancer medicine. Br J Cancer *102*, 693-703.

Stenson, P. D., Mort, M., Ball, E. V., Shaw, K., Phillips, A., and Cooper, D. N. (2014). The Human Gene Mutation Database: building a comprehensive mutation repository for clinical and molecular genetics, diagnostic testing and personalized genomic medicine. Human genetics *133*, 1-9.

Stites, E. C., and Ravichandran, K. S. (2012). Mechanistic modeling to investigate signaling by oncogenic Ras mutants. Wiley Interdiscip Rev Syst Biol Med *4*, 117-127.

Tartaglia, M., Pennacchio, L. A., Zhao, C., Yadav, K. K., Fodale, V., Sarkozy, A., Pandit, B., Oishi, K., Martinelli, S., Schackwitz, W.*, et al.* (2007). Gain-of-function SOS1 mutations cause a distinctive form of Noonan syndrome. Nat Genet *39*, 75-79.

The Cancer Genome Atlas Netwrok (2011). Integrated genomic analyses of ovarian carcinoma. Nature *474*, 609-615.

Trampont, P. C., Tosello-Trampont, A. C., Shen, Y., Duley, A. K., Sutherland, A. E., Bender, T. P., Littman, D. R., and Ravichandran, K. S. (2010). CXCR4 acts as a costimulator during thymic beta-selection. Nature immunology *11*, 162-170.

Tyner, J. W., Erickson, H., Deininger, M. W., Willis, S. G., Eide, C. A., Levine, R. L., Heinrich, M. C., Gattermann, N., Gilliland, D. G., Druker, B. J., and Loriaux, M. M. (2009). High-throughput sequencing screen reveals novel, transforming RAS mutations in myeloid leukemia patients. Blood *113*, 1749-1755.

Williams, V. C., Lucas, J., Babcock, M. A., Gutmann, D. H., Korf, B., and Maria, B. L. (2009). Neurofibromatosis type 1 revisited. Pediatrics *123*, 124-133.

Yang, F. C., Chen, S., Clegg, T., Li, X., Morgan, T., Estwick, S. A., Yuan, J., Khalaf, W., Burgin, S., Travers, J.*, et al.* (2006a). Nf1+/- mast cells induce neurofibroma like phenotypes through secreted TGF-beta signaling. Hum Mol Genet *15*, 2421-2437.

Yang, F. C., Chen, S., Robling, A. G., Yu, X., Nebesio, T. D., Yan, J., Morgan, T., Li, X., Yuan, J., Hock, J.*, et al.* (2006b). Hyperactivation of p21ras and PI3K cooperate to alter murine and human neurofibromatosis type 1-haploinsufficient osteoclast functions. J Clin Invest *116*, 2880-2891.

Young, A., Lou, D., and McCormick, F. (2013). Oncogenic and wild-type Ras play divergent roles in the regulation of mitogen-activated protein kinase signaling. Cancer Discov *3*, 112-123.

Zi, Z. (2011). Sensitivity analysis approaches applied to systems biology models. IET systems biology *5*, 336-336.

Table S1, related to Figure 4. Ras pathway mutations from the CCLE dataset that were analyzed as part of this study.

The CCLE dataset analyzed was reported in Barretina J, et al, 2012.

Table S2, related to Figure 4. Ras pathway mutations from the TCGA dataset that were analyzed as part of this study.

The TCGA dataset analyzed was reported in Kandoth C, et al, 2013.

Table S3, related to Figure 4. NF1 mutations analyzed in this study that have also been observed in patients with neurofibromatosis.

NF1 mutations analyzed in this study were compared with reported NF1 mutations from neurofibromatosis patients listed in the Human Gene Mutation Database (Stenson et al., 2014).